DEPARTMENT OF CIVIL ENGINEERING

Water Resources Research Group

UNIVERSITY OF SALFORD

Department of Civil Engineering, University of Salford, Salford, M5 4WT,
U.K. Telephone: 061-736 5843. Telex: 68741 (Salcel). Fax: 061-745 7027.

ARIP REPORT No. 4

~~~~~~

ANGLIAN RADAR INFORMATION PROJECT

~~~~~~

ANGLIAN RADAR INFORMATION PROJECT

REPORT NO. 4

Aspects of Precipitation Observation and Quantitative Estimation with Weather Radar

Water Resources Research Group
Department of Civil Engineering
University of Salford
Salford, M5 4WT

Report prepared by

K.A. Tilford and Prof. I.D. Cluckie
August 1991

Contents

List of figures

List of tables

Chapter 1. Introduction

This is the fourth report to be submitted as part of the Anglian Radar Information Project (ARIP).

The main purpose of the report is to provide an insight into the theoretical background of weather radar observation and quantitative estimation of precipitation. Chapter 2 presents a brief introduction to the basic principles underlying precipitation observation and quantitative estimation using weather radar, whilst chapter 3 covers in some detail those factors which influence the quantitative estimation of precipitation intensities.

The emphasis is on those aspects which are directly relevant to and will aid understanding and comprehension of, quantitative precipitation estimation and will therefore enable the radar adjustment schemes developed during the course of the Anglian Radar Information Project (see ARIP Report 5) to be placed in a realistic and proper context. Hence topics such as beam attenuation, ground clutter, earth curvature, anomalous propagation and bright-band are all discussed in a theoretical manner.

The U.K. weather radar network, the characteristics of the radars operating as part of this network, and the radar products disseminated by the Meteorological Office are included in the Report appendices. In particular, aspects of radar data resolution in space, time and intensity, are discussed.

Chapter 2. Basic Principles of Radar Precipitation Estimation

This chapter briefly describes the theoretical principles and concepts underlying radar precipitation observation and estimation. It is hoped therefore that this chapter will enhance the readers comprehension of the material covered not only in the rest of the report but also in other ARIP Reports (notably ARIP Report 5), thereby enabling the reader to place it in a realistic and proper perspective. The treatment is not rigorous and for more detailed information the reader should refer to any of the references provided in the chapter. The authors particularly recommend Battan (1973), very much a seminal work on weather radar, Clift (1985), a WMO report in which essential information is presented succinctly, and Collier (1989) a text which focuses on the hydrological applications of weather radar.

2.1. Background

Radar is an echo-sounding device in which the range of a target is determined from the time taken for an electromagnetic pulse to travel to and return from the target after reflection. The major hardware components of a typical weather radar system are illustrated in figure 2.1. The trigger produces a pulse of electromagnetic energy which is fed to the transmitter. The transmitter is the most critical component of the system, and converts the pulse to the required wavelength. The electromagnetic energy is concentrated into a narrow beam and radiated from the antenna. The antenna is parabolic resulting in a beam which diverges - (a pencil-like near parallel-sided beam could be achieved but is undesirable since only a very small volume of the atmosphere would be sampled). The antenna also receives the returned energy and returns it to a receiver module. The signal is processed and the meaningful information analysed. An idealised radar beam, conic in section, inclined by an elevation α, of width θ and inclined at angle α, under conditions of normal atmospheric propagation is shown in figure 2.2.

The maximum beam power is along the axis perpendicular to the face of the antenna, and as the angle away from this increases the power decreases (rapidly). The beamwidth is defined as the angle between those directions in which the intensity of the beam is at least one-half the maximum. The importance of beamwidth on the observation of rainfall is discussed in section 3.1.4. Small subsidiary beams (side-lobes) appear either side of the main beam (with decreasing strength as the angle from the central axis increases. Figure 2.3 shows a cross-section through a radar beam.

The antenna is also used for detecting the returned energy, and to accommodate this the radar operates in an emission-reception cycle; first emitting short pulses and then waiting until these are received (the waiting period is minimal since electromagnetic radiation travelling at the speed of light will cover 400 km in approximately 0.0013 seconds). The intensity of the returned energy may be as little as 10^{-17} the intensity of the emitted pulses due to attenuation and absorption (described more fully in section 3.1.3).

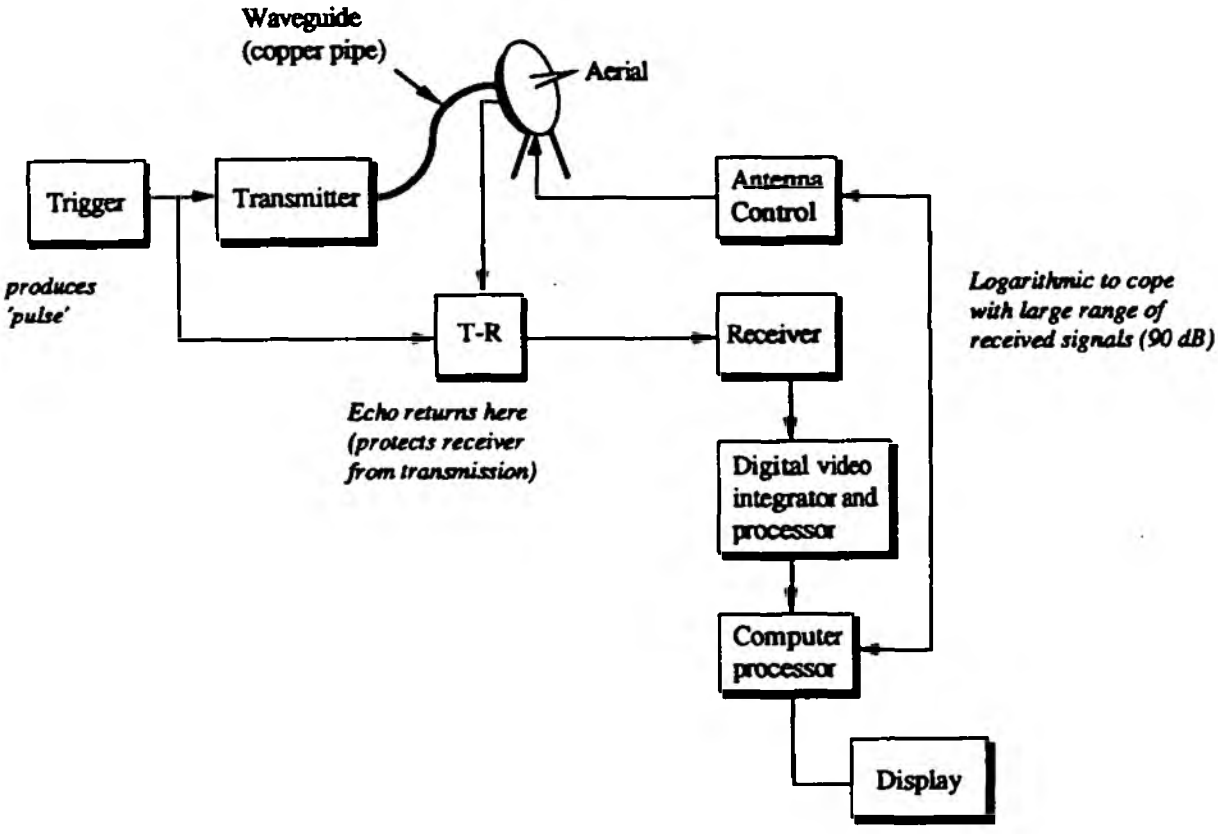

Figure 2.1: Main components of a weather radar system

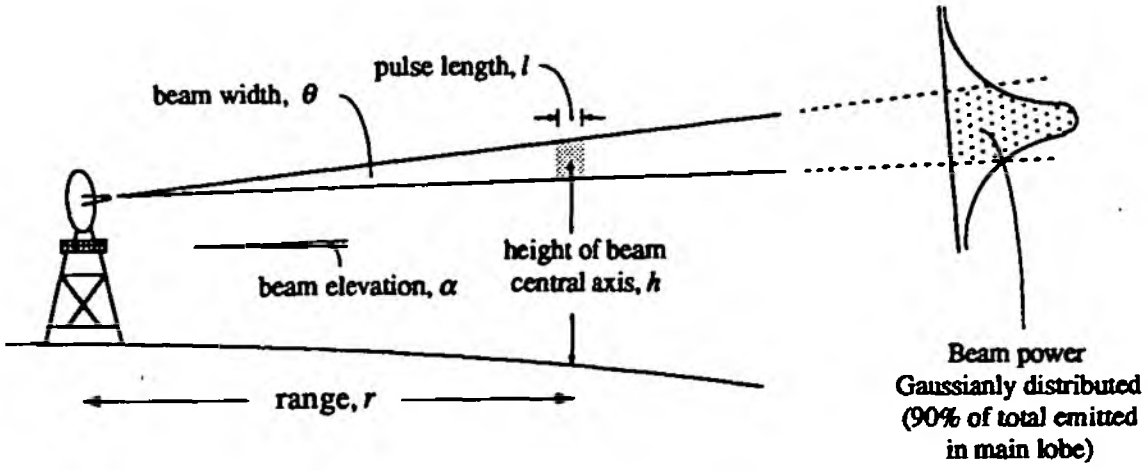

Figure 2.2: Geometry of an idealised pulse volume

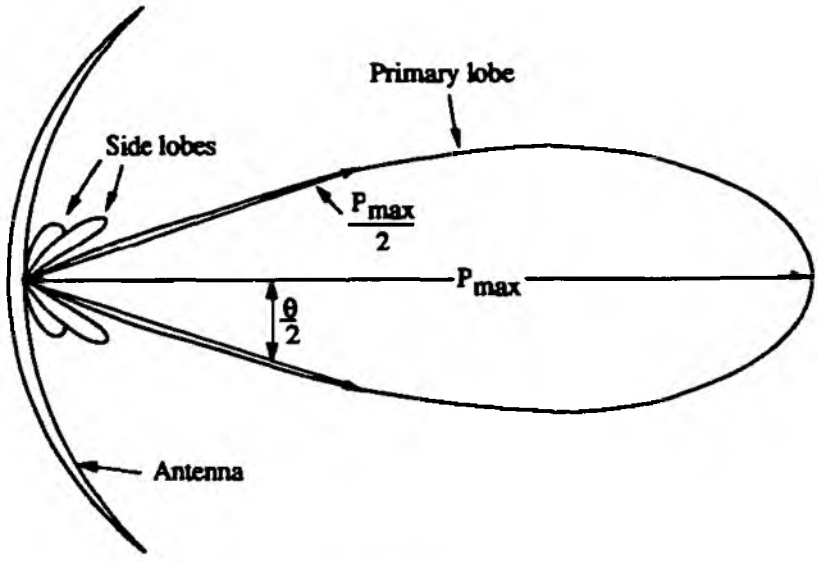

Figure 2.3: Cross-section of a radar beam from a parabolic reflector (Clift, 1985)

The amount of energy back-scattered from the hydrometeors depends upon the number of particles within the pulse volume of the radar beam, their size, composition, relative position, shape and orientation. When the drop diameter is small compared to the wavelength, i.e. the electrical size of the droplets α is less than 0.13 (where $\alpha=\pi D/\lambda$), scattering known as Rayleigh scattering applies and the back scattering cross section σ is given (after Battan, 1973) by:

$$\sigma_i = \frac{\pi^5}{\lambda^4} |K|^2 D_i^6 \qquad \text{(eq. 2.1)}$$

Hence, the scattering cross section is proportional to the sixth power of the drop-size diameter. $|K|^2$ is a function of the refractive index of the scattering particles, and is approximately five times greater for water (0.93) than for 'dry' ice (0.197).

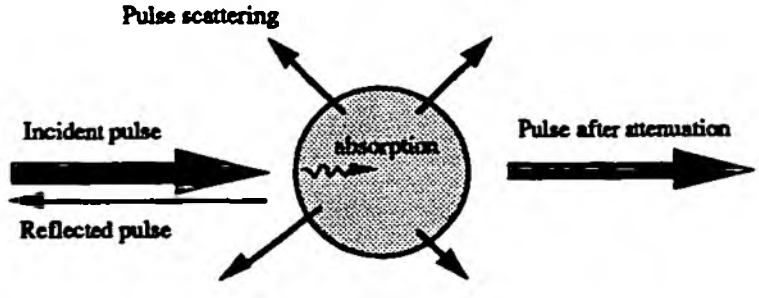

Figure 2.4: Radar pulse scattering, attenuation and reflection

When the entire beam cross section is considered, the average power received P_r is the sum of the contribution of individual scatterers, and is represented by a form of the fundamental radar equation:

$$P_r = \frac{C}{r^2} |K|^2 \sum_{i=1}^{n} D_i^6 \qquad \text{(eq. 2.2)}$$

It is not practical to measure operationally ΣD^6 i.e. the drop-size distribution at the ground and to convert this to a volume distribution by means of drop fall speeds, because rainfall is never composed of droplets of uniform size. Furthermore, the drop-size distribution cannot be determined theoretically. Thus, an empirical relationship between rainfall intensity and ΣD^6 is utilised. ΣD^6 is known as the radar reflectivity Z (usually expressed in volume units $mm^6\ m^{-3}$).

$$P_r = \frac{C}{r^2} |K|^2 Z \qquad \text{(eq. 2.3)}$$

Z is empirically related to the rate of rainfall by $Z=aR^b$ where R is the rainfall intensity and a and b are constants. This is known as the Z-R relationship, a relationship fundamental in radar precipitation estimation. C is known as the radar constant and can be accurately determined for a given radar system, being a function of wavelength, beamwidth, pulse length, transmitted power, antenna gain and the target refractive index.

Equation 2.3 is subject to numerous assumptions including (after Collier, 1989):

- Rayleigh scattering theory is applicable.
- The pulse volume is completely filled with randomly scattered spherical particles.
- The reflectivity factor Z is uniform throughout the sampled pulse volume.
- $|K|^2$ is the same for all particles (i.e. either all water droplets or all ice particles).
- Absorption of the transmitted signal by ground clutter in the beam is negligible.

The values of a and b depend upon the rainfall type. Commonly used values (determined empirically) are a=200 and b=1.6 (Marshall and Palmer, 1948). Use of this relationship, varying a and b as appropriate is unfortunately not straightforward due to both radar properties and precipitation / cloud structure. The Z-R relationship is directly discussed further in section 3.4.1 though the contents of the following chapters should be considered in the context of the comments made in this section.

2.2. An Illustrative Example

The basic principles described in the preceding paragraphs are illustrated with the following example

(after Grayman and Eagleson, 1970). In this example the radar is observing a storm that extends from range r_1 to r_2 in a particular direction (azimuth) from the radar. A pulse is emitted from the radar at time $t=0$ and spreads out in a cone shape with beamwidth θ (figure 2.5[i]). As the beam diverges, the pulse of energy spreads out over an ever increasing area so that the power per unit area falls inversely proportionally to the square of the range (figure 2.5[ii]). When the pulse encounters the storm, the raindrops reflect some energy back toward the antenna and at time $2t_1$ (the time taken for the pulse to travel distance $2r_1$ at the speed of light) the antenna starts to receive meaningful signals. This continues until time time $2t_2$ at which point the outer extent of the storm has been reached. Once the signals have been adjusted (normalised) to account for range they can be displayed graphically. The trace in figure 2.5(iii) shows how the signals would appear on an A-scope (one of the most elementary of indicators which operates like a test oscilloscope used in physics or electronics laboratories). On this scope, the abscissa is the range whilst the ordinate is the intensity of the normalised received power. The signal prior to $2t_1$ and after $2t_2$ is 'noise' that is always present.

2.3. Information Display

The example in section 2.2 introduced one of the most elementary ways in which radar derived rainfall intensity can be displayed, the A-scope. Other types of radar displays presenting different information concerning storm characteristics have developed. The most common are described below and illustrated in figure 2.6.

By rotating the antenna in a circle at a fixed beam elevation (azimuth scanning), the horizontal extent of the entire storm may be displayed. The most extensively used indicator on weather radars is the plan-position indicator (PPI) which displays a plan view of the signals received on a polar coordinate system (though conversions are commonly applied to transform the data to a cartesian coordinate representation). See figure 2.6(i).

Another commonly used radar display is the range-height indicator (RHI) (figure 2.6[ii]). This type of presentation is used with radar devices with antenna's possessing the capability to scan vertically. In this mode, the vertical angle of the antenna is varied through the operational range of the device enabling the vertical profile of the storm to be examined for any particular azimuth. Height finding radars are particularly useful in studies of cloud and precipitation growth and have been used extensively in cloud physics research.

A display technique which incorporates procedures from both the PPI and RHI modes is the constant altitude PPI (CAPPI), a technique first developed by the Stormy Weather Group at McGill University (Marshall, 1957; East and Dore, 1957). In this display, rainfall intensity for the radar is displayed in a plan manner as with the PPI display, but all the reflectivity data are derived from observations made at the same altitude by compositing segments of scans made at different elevations (figure 2.7).

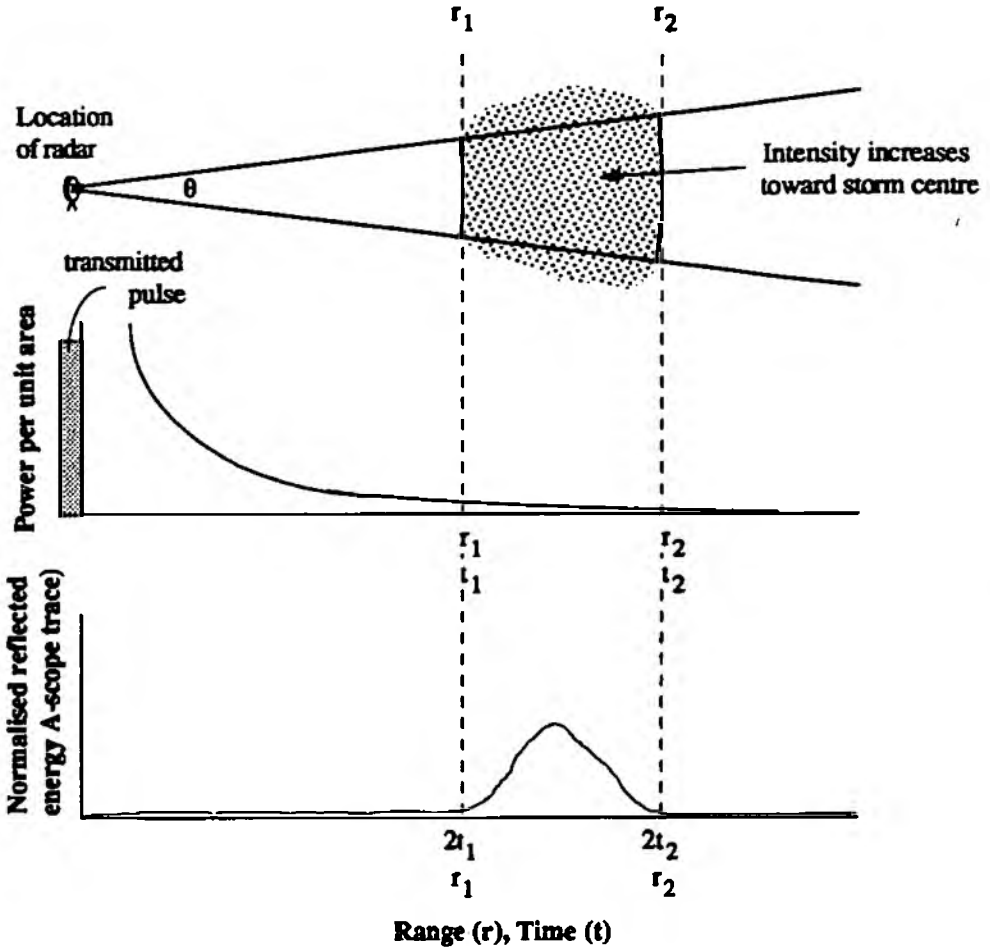

Figure 2.5: Essentials of radar detection of precipitation (adapted from Grayman and Eagleson, 1970)

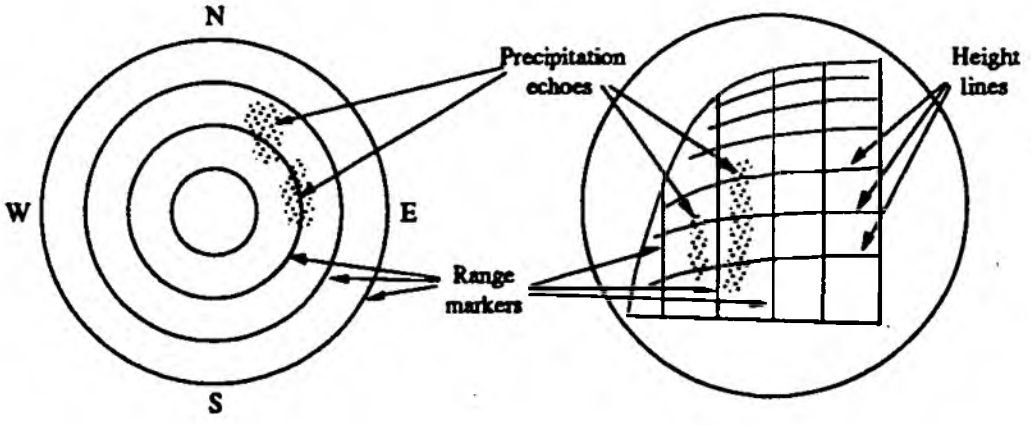

Figure 2.6: Common radar display modes (Battan, 1973)

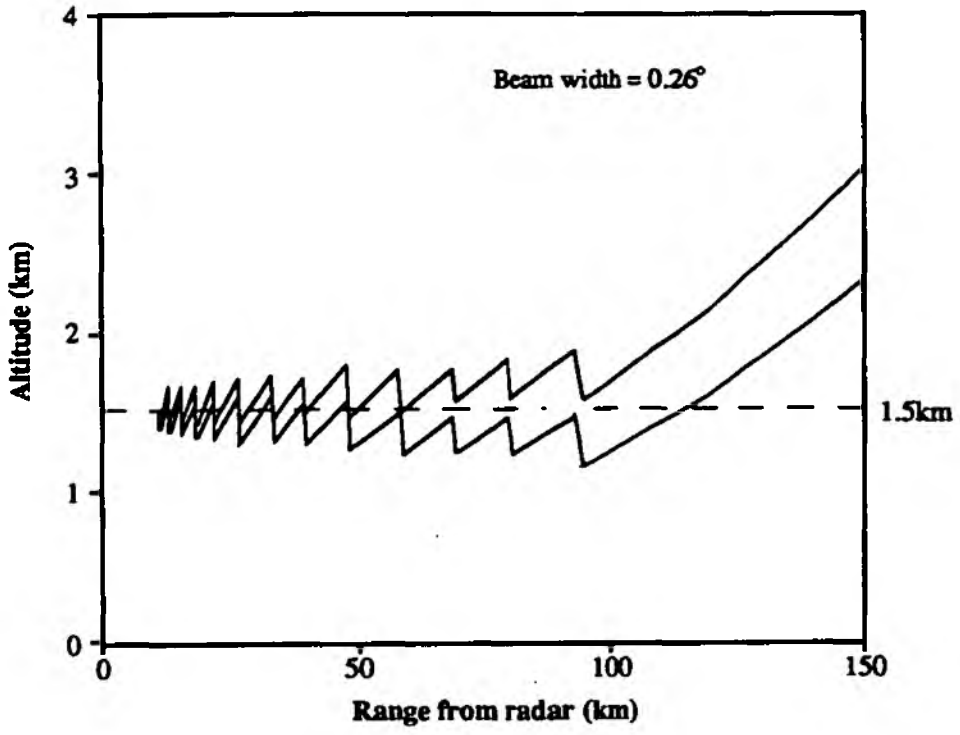

Figure 2.7: Beam segmentation and composition to produce a 1.5 km CAPPI

Chapter 3. Factors influencing Quantitative Radar Precipitation Estimation

A major benefit of weather radar is the capability to estimate precipitation in real-time over a large area from a single location. However, there are a number of problems associated with radar precipitation estimation at all ranges but particularly at longer ranges. This chapter presents the most important of these. The chapter is sub-divided into four main sections: the first section covers radar hardware influences on estimation accuracy; the second discusses errors which may arise due to radar siting and the interaction of the radar beam with the local topography; the third section covers a range of further accuracy factors primarily due to beam propagation characteristics and the height of the radar beam above the ground; finally the fourth section covers problems posed by variations in reflectivity / rainfall relationship and the vertical reflectivity profile.

3.1. Factors due to Radar Hardware

A number of important factors are due to the radar system hardware. It is important that these are considered and appropriate for the prevailing circumstances. The most important of these are discussed in this section.

3.1.1. Dynamic Range

Dynamic range is a measure of the range of precipitation intensities that can be handled by the radio receiver without distortion of their relative values. If the dynamic range is too small, either light precipitation will not be detected or heavy precipitation will be reduced in apparent intensity. Dynamic range is consequently related to the physical rainfall process of the region the radar is sited, for example, the dynamic range required in a temperate climate will differ considerably from that required in a tropical region. Accurate determination of the required dynamic range is however problematical since measurement of maximum instantaneous rates of precipitation poses a major instrumentation problem, despite advances in rapid response raingauge technology. Current radar technology is such that it is possible to manufacture a receiver (80 dB) which can handle mean precipitation intensities in the range 0.1 mm h^{-1} to 256 mm h^{-1}.

3.1.2. Radar Wavelength

The wavelength at which the radar operates is inter-related with a number of other radar characteristics. Between them these properties determine the extent to which quantitative precipitation estimation accuracy is likely to be affected. The degree of inter-relation makes it difficult to consider any one parameter in isolation. The following sections refer repeatedly to wavelength and detailed discussions are left until the appropriate section, however it is useful to summarise in a general manner radar wavelength with respect to hydrometeorological applications

(table 3.1).

Table 3.1: Radar system characteristics and hydrometeorological applications

'Band'	Wave length	Frequency range (MHz)	Comments
L	20 cm	30 000	No hydrometeorological applications.
S	10 cm	2700 - 3000	Best suited to regions where heavy rainfall occurs and attenuation may be a problem (section 3.1.2), e.g. tropical areas. Requires a large reflector to produce a small beamwidth (table 2.2).
C	5.6 cm	5300 - 5700	Affords good compromise between hardware cost and precipitation estimation performance for most hydrometeorological applications in temperate regions. Qualitative range limited to about 200 km (quantitative range about half). (Total cost for a working system in the region of £ 1 million (1990 prices).
X	3 cm	9300 - 10 000	In the past used mainly in polar and near polar regions where attenuation is not a major problem. Currently receiving interest for limited range applications (e.g. urban applications) in temperate regions, where range is limited to approx 35 km. Cost of a complete working system approx. £ 100 000 (1990 prices).
K	0.8 cm	37 500	Not in widespread use except in some eastern European dual wavelength systems where it is combined with a longer wavelength. Can detect the smallest cloud particles and has been used to study cloud microphysics.

3.1.3. Beam Attenuation

Beam attenuation can be sub-divided into three categories: attenuation due to range, attenuation due to absorption/scattering by atmospheric gases, liquids and solids; and attenuation due to radome wetting. These are discussed in the following section. Typical attenuation amounts due to the first two processes are summarised in table 3.2.

Range attenuation is accommodated by a parameter (r) in the fundamental radar equation for the scattering of electromagnetic pulses by an extended target (section 2.1, equation 2.2). The equation demonstrates that the received signal power is inversely proportional to the square of the range of the target. Range attenuation correction attempts to make a given echo target at 100 km appear the same as if it were at 10 km. This can either be achieved via radar hardware (usually known as swept gain) or by range normalisation software.

A further parameter in the radar equation is the attenuation factor K, energy loss of electromagnetic waves travelling through the atmosphere due to absorption and scattering. Of the atmospheric gases, oxygen and water vapour both attenuate electromagnetic radiation though in neither case is it significant. More important is attenuation by liquid and solid particles, attenuation due to precipitation being by far the most important (Joss and Waldvogel, 1989 suggest that for 5.6 cm wavelengths, if the radar beam travels for some distance along the melting layer or bright-band layer attenuation amounting to several times that found in rain layer below may occur).

Table 3.2: Attenuation due to absorption and scattering

Oxygen (1)	(2)	0.008 - 0.01 dB km^{-1}	1.6 - 2.0 dB at 100 km
Water vapour	3 cm	0.01 dB km^{-1} (3)	2.0 dB at 100 km
	10 cm	0.0002 dB km^{-1}	0.04 dB at 100 km
Cloud - (water droplets) (4)	3 cm	0.1 dB km^{-1}	1.6 - 2.0 dB at 100 km
	10 cm	0.01 dB km^{-1}	1.6 - 2.0 dB at 100 km
Cloud - (ice crystals) (5)	3 cm	0.004 dB km^{-1}	0.8 dB at 100 km
	10 cm	0.0008 dB km^{-1}	0.16 dB at 100 km

Precipitation (attenuation units dB)	Intensity (mm h^{-1})	10 cm	5 cm	3 cm
	0.5	0.0003	0.002	0.006
	1.0	0.0006	0.004	0.014
	5.0	0.003	0.030	0.122
	10.0	0.006	0.066	0.302
	50.0	0.03	0.430	2.500
	100.0	0.06	0.962	6.160

(1) at sea level pressure
(2) nearly constant for wavelengths in the range 3 to 10 cm
(3) assuming 7.5 g m^{-3} at 1000 hP pressure
(4) assuming a water vapour content of 1 g m^{-3} (high for most clouds)
(5) assuming an ice crystal content of 1 g m^{-3}

Attenuation due to precipitation is inversely related to the wavelength of the microwaves. For a wavelength of 10 cm, attenuation is small except at very high rainfall rates, but at shorter wavelengths the attenuation becomes severe. This is illustrated in figure 3.1.

Radomes are the protective housing for the radar antenna, often constructed of a rubber-like material which is kept inflated by air pressure or (more commonly now) fibre-glass panels

supported by a space-frame. Radomes are designed to protect the antenna from precipitation, wind and pollution, enable servicing in all weather conditions, and also rule out problems in antenna rotation speed due to wind. A disadvantage is the additional beam attenuation the radome introduces due to the radome material (though this is constant and is easily correctable), but also to water droplets collecting on the exterior surface. Unfortunately little work has been conducted on the latter and it is rarely considered.

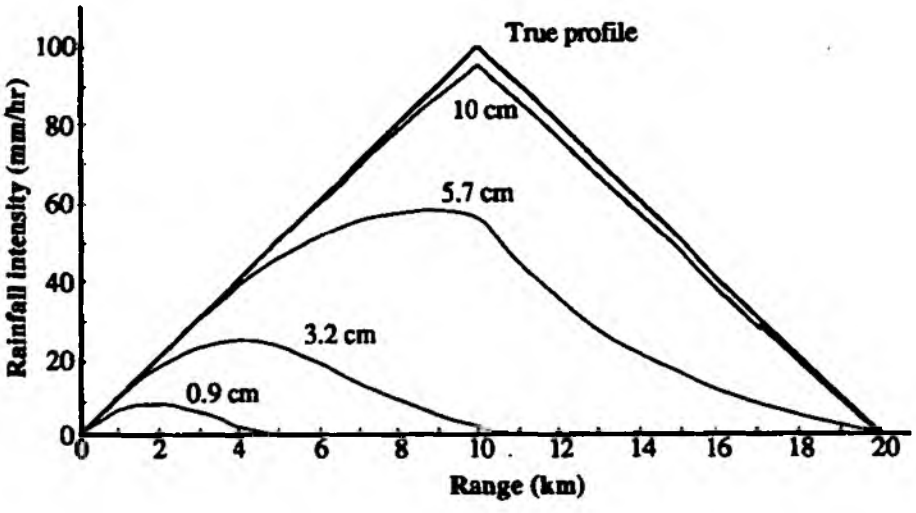

Figure 3.1: Modification of the profile of a shower 20 km in width in which the intensity of the precipitation varies by 10 mm/hr/km (adapted from Treussart, 1968)

Beam attenuation is a major factor in the design of weather radar hardware. Consequently, 10 cm radars have found application in tropical areas where intense rainfall is relatively commonplace, whilst 5.6 cm radars are generally assumed to be the most appropriate general purpose device for temperate latitudes. Recent interest has focussed on the application of low cost 3 cm wavelength devices for use in urban areas where the quantitative range is restricted to 30 km (refer also to table 3.1).

3.1.4. Beamwidth

The concept of radar beamwidth and side-lobes was introduced in section 2.1. For hydrometeorological applications a beamwidth of 1° is regarded as near optimal. This figure is not solely due to beam propagation arguments (if only these were considered it is highly likely that a narrower beamwidth would be better, e.g. 0.5°), but also to practical and economical considerations. The strength of the return signal received at the antenna is directly proportional to the aperture diameter and will be maximised with a large antenna. However, practical as well as economic constraints mean that for hydrometeorological scanning radars the antenna diameter is

limited to about 7 m diameter. For a circular parabolic reflector the beamwidth θ (in radians), antenna diameter d, and wavelength λ are related by $\theta=1.2\lambda/d$, so for a 10 cm wavelength system this results in a beamwidth of about 1°. Beam diameter-range and reflector diameter-wavelength relationships for different beamwidths are shown in table 3.3.

Table 3.3. Beam diameter-range and reflector diameter-wavelength relationship for different beamwidths

Beamwidth (degrees)	Approximate diameter of main beam lobe (m)			Reflector diameter required (m) for different wavelengths		
	50km	100km	150km	10 cm	5.6 cm	3 cm
0.5	436	873	1309	13.8	7.7	4.1
1.0	873	1745	2618	7.3	3.7	2.1
2.0	1745	3490	5236	3.4	1.9	1.0

Reducing the system wavelength results in a smaller beamwidth, so a 3 cm wavelength system can provide a 1° beamwidth with a 2 m reflector. This is the reason that the X-band systems discussed in section 3.1.2 (see also table 3.1) are both small and relatively cheap. However attenuation must also be considered in conjunction with the beamwidth and antenna size.

One of the practical consequences for rainfall observation is that two targets separated by less than the beamwidth in angle cannot be resolved in space by the radar. The example in figure 3.2 illustrates this by comparing the observations of two rainfall cells by two different radar systems, the first (case 1) operating a beamwidth θ, and the second (case 2) having a smaller beamwidth ($\theta/2$). The two storm cells move towards the radar with a constant speed and with a constant cell separation. In the first case, the beamwidth is such that at range r_1 (time t_1) the radar is unable to resolve the individual cells, individual resolution only occurring as the cells move toward the radar and as the beamwidth narrows (r_2, t_2), (thereby giving the misleading impression that a previously continuously echo belt has begun to split up into separate cells). In contrast, the smaller beamwidth system correctly resolves the cells at all ranges.

The spatial resolution required for any particular hydrological application remains to a large extent unresolved though it is clear from recent (and continuing) research of groups in Hanover, (Germany), Paris (France) and by various groups in the U.K that applications in the urban environment have more stringent requirements than rural applications. Haggett (1989) cites an example of spatial averaging introducing errors in a local convective storm over south-east London, the observed rainfall intensity varying from 13.5 mm/hr to 21.5 mm/hr depending on whether 5 km or 2 km radar data were referred. In a detailed analysis of the spatial resolution effects on three storm events, Yuan (1991) observes that areally averaged rainfall amounts derived from 2 km and 5 km data are very similar, (maximum relative deviations of 2 %) though the differences become

much more significant when distributed effects at a 2 km^2 scale is considered (relative deviations ranging from 9 % to 26 %). A summary of the results is shown in table 3.4.

Side-lobes (see section 2.1) produce unwanted echoes from close-range targets even when the main beam is elevated in order to avoid these permanent echoes falling within the main beam, and this tends to prevent precipitation estimation within about 5 km range of the radar.

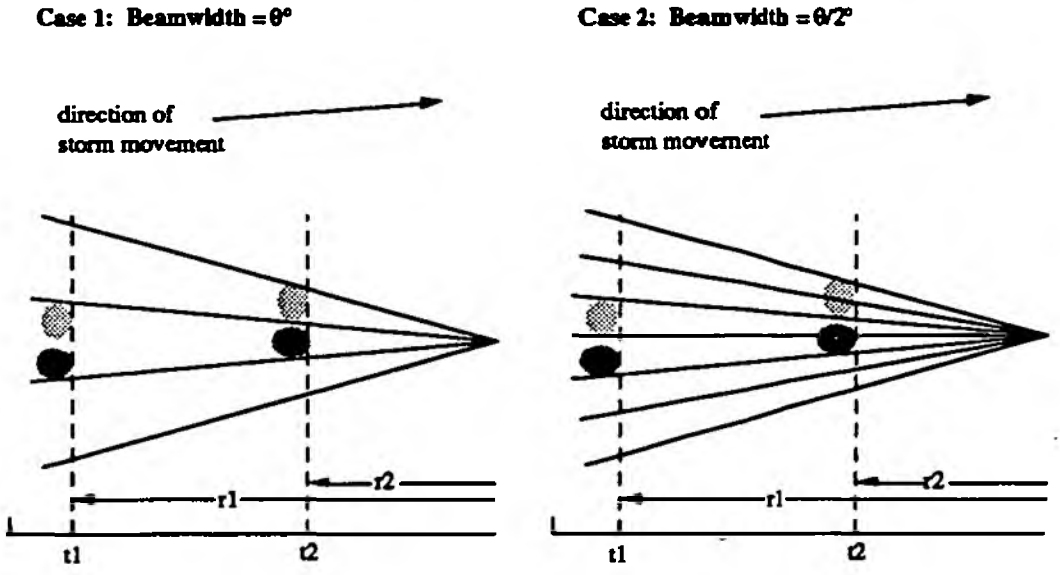

Figure 3.2: Influence of beamwidth on spatial resolution (plan view of radars)

Table 3.4. Spatial variation effects on radar rainfall data (source: Yuan, 1991)

Event date	Duration	Mean rainfall amounts (mm)	
		2 km	5 km
23rd May 1988	00:00 - 24:00	7.3	5.2
18th Aug 1988	00:00 - 24:00	16.2	13.2
1st Sept 1988	00:00 - 24:00	2.6	3.5

3.2. Factors due to Radar Siting

A number of problems are associated with the siting of the radar in conjunction with the beam propagation properties. Measures to minimise and cope with these can be taken but it is impossible to remove them completely.

3.2.1. Permanent Echo

An idealised beam path is shown in figure 2.2. In practice, both the main part of the radar beam and/or the side lobes (see figure 2.3) may encounter ground targets causing strong persistent echoes which if uncorrected can be misinterpreted, either as rainfall when there is none, or higher intensity rainfall than really exists. Contamination of the reflectivity signal in this manner can be due to interference directly from the ground or from ground-based objects such as towers, trees and radio masts. This permanent echo or ground clutter constitutes a significant problem in radar rainfall detection and surface rainfall estimation. It is worth noting the observations of Joss and Waldvogel (1989a) that ground clutter echo strength is almost independent of wavelength.

Because of the seriousness of the ground clutter problem, a major factor in the siting of weather radars in all but the flattest, obstruction free regions (e.g. see Van den Assems paper, 'Calibration of Weather Radar Data in the Netherlands', 1989) is an obstruction-free horizon. However, whilst a site with an excellent horizon can minimise clutter returns, total removal is never possible. Consequently considerable effort has been channelled into ground clutter identification and correction procedures.

A widely utilised technique is to use a ground clutter pattern or permanent echo map. Because in general the spatial distribution of ground clutter will be stable, a digitised map of echo distribution observed in dry, stable atmospheric conditions can be produced. The map stores the locations of cells where the echo exceeds the noise threshold of the radar. When data are collected in the presence of precipitation, the clutter map is used in a 'look-up' manner to identify the areas affected by clutter, and observations made in these regions are discarded and replaced by a value interpolated (usually linearly) from observations made in surrounding clutter-free areas (azimuth-interpolated) and/or from higher beam elevations (elevation-interpolation).

In general this technique works well, though under conditions of orographic enhancement, substantial topographical changes within the affected areas can result in non-linear changes in rainfall (Collinge, 1989) introducing an additional source of error into the interpolation. More general shortcomings are: clutter maps assumes a constancy in the behaviour of the clutter, an assumption that can be violated as meteorological conditions change the atmospheric refractive index and thus beam propagation; objects moistened by rain produce different reflections than when dry (van Gorp, 1990).

Ground clutter tends to be more of a problem close to the radar where the beams are closer to the ground than at longer range. However, even at the longer ranges and especially in hilly or mountainous regions, ground clutter may still present a serious problem (recent examples of work on the problems of radar measurement in mountainous regions are presented by Galli and Joss, 1989 [Switzerland]; and by Tateya *et al*, 1989 [Japan]), especially at low beam elevations and with large beamwidths. At the shorter ranges, switching to a higher elevation beam may provide a solution (if the beam height is not too high) since it prevents the main lobe from intersecting the

ground. However, beam infilling in this manner accentuates range associated problems of radar by increasing the height of the beam used to determine precipitation amounts (see section 3.2.2).

The approach adopted in the U.K. to overcome ground clutter is similar to the 'sectorized hybrid scan' procedure used in the United States (Shedd *et al.* 1989; Hudlow *et al.* 1989). Radar horizons determined from theodolite site surveys (to determine obstructions from buildings, trees etc.) and from computer processing of digitised ground relief data (topographical mapping) are combined to determine overall sight horizons around the radar site. These are then used to determine the appropriate beam elevations for all azimuths and range.

3.2.2 Screening

As well as producing permanent echoes, interception of the beam also causes occultation or screening of the beam such that only a fraction of the total beam power extends to ranges beyond the obstruction. This is illustrated in figure 3.3.

Partial blocking of the radar beam occurs in areas at ranges beyond blockages produced by hills. In addition to the ground clutter this causes, echoes from precipitation observed beyond will be weaker than they would otherwise have been had the beam been complete. It is possible to compensate objectively for such screening or occultation provided that at least 40% of the beam is unobstructed (Harrold *et al*, 1974), in which case the correction factor applied is a function of the percentage of the beam cross sectional area obstructed (stored as a digitised look-up map), thereafter the radar data are replaced by interpolated values (as described in the previous section). Andersson (1989) observes from experience in Norway that corrections for partial blocking become increasingly unreliable as range increases and tend to be most effective at short range.

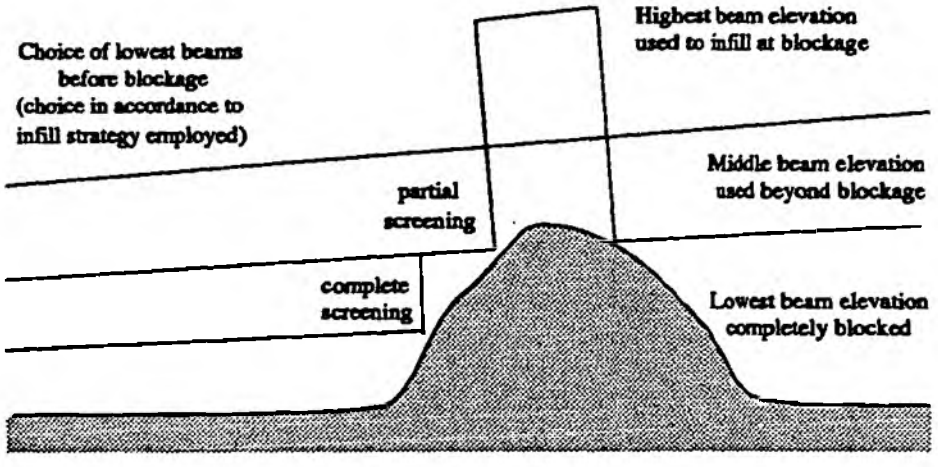

Figure 3.3: Beam infilling in the presence of ground clutter due to terrain blocking

3.3. Accuracy Factors

The following factors all have a direct (and often major) impact on the error of the radar precipitation estimation.

3.3.1. Beam Infilling

The Z-R relationship assumes that the radar beam is completely filled by precipitation scatterers. When this is not so, for example in localised showers, the reflected energy will be less than the rate of precipitation will justify; as a result an underestimate will be made. At a range of 100 km, a beam with a width of 1° will have a circular cross-section of diameter 1.75 km. For the Z-R relation not to be violated, the scattering particles should be uniformly distributed in size and number throughout the volume. This is never likely to be precisely true, though the narrower the beamwidth the more accurate the assumption becomes. The greater the range, the greater the chance that the beam will be incompletely filled. A practical effect of incomplete filling is that showers at long range may appear to become more intense as they approach the radar whereas in fact this is only because they are merely filling a greater proportion of the beam volume. The need to have the beam filled is one of the major reasons for restricting the range of observations, and for using the smallest practicable beamwidth. Depth and type of precipitation is a therefore a major factor of estimation accuracy, especially at long range.

3.3.2. Earth Curvature Effects

The path followed by a radar beam depends on the refractive index structure of the atmosphere. This is vertically stratified so that radar waves travelling through the atmosphere follow curved rather than straight paths. Usually, in 'normal atmospheric conditions' the beam path is close to circular with a radius 4/3 the radius of the Earth (but see section 3.2.3 - anaprop). This combined with Earth curvature causes the path of the beam to diverge from the Earth's surface with two major consequences: there is an area between the bottom of the beam and the Earth's surface in which neither detection nor measurement is possible (an area which increases with range and limits viable radar range), and the beam will inevitably pass through the melting layer.

Figure 3.4 shows the height of radar beam centres above the surface of the Earth (assuming the radar is at mean sea level), for the beam elevations utilized by the Chenies radar. Beam height is determined using the so-called 'four-third's Earth approximation' shown in equation 3.1. The equation models the trajectory of a radiowave through a standard atmosphere, allowing for both the refraction of the ray due to the atmosphere and the curvature of the Earth.

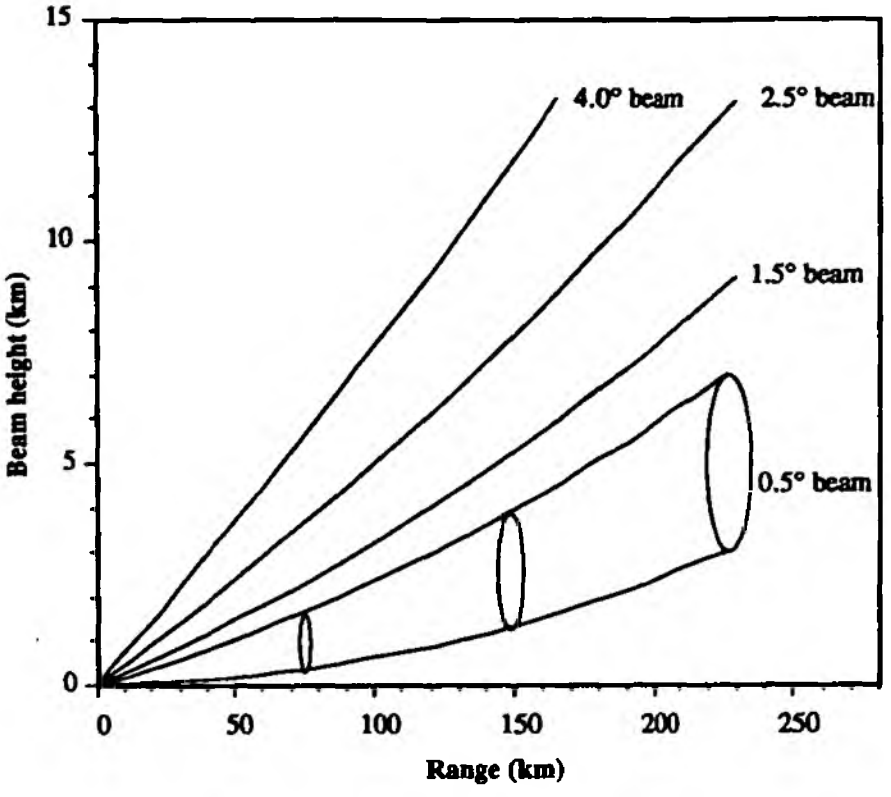

Figure 3.4: Beam height and conical diameter (of the 0.5° beam) as a function of range (beamwidth assumed as 1°)

$$h(r, \theta) = r\left[\frac{3r}{8E}\cos\theta + \sin\theta\right] \qquad \text{(eq. 3.1)}$$

where θ is the elevation of the radar beam axis (in radians) and E the radius of the Earth (km).

The effects of divergence between the beam and the Earth's surface on estimates of surface precipitation are:

- low level precipitation may be missed altogether;
- low level precipitation enhancement may take place below the beam;
- low level evaporation may occur;
- precipitation may drift horizontally below the beam.

These problems (together with the bright-band phenomenon discussed in section 3.4.2) result in some of the most serious errors associated with radar precipitation estimation, and it is towards these problems in particular that improved adjustment procedures using, for example, a number of local telemetering raingauges address.

3.3.3. Anomalous Propagation

As mentioned in section 3.3.2, the path followed by a radar beam depends on the refractive index structure of the atmosphere. This is vertically stratified so that radar waves travelling through the atmosphere follow curved rather than straight paths. The following paragraph describes those factors that influence the actual path of the beam, what 'normal conditions' are, and the consequences of 'abnormal conditions'.

The curvature of a radar beam path depends on the rate of change of the refractive index (n) with height (z), n being a function of pressure, temperature, and water vapour pressure. So, if the vertical profile of all is known, the path of the beam can determined. In the atmosphere n is so close to unity for microwave frequencies so that a modified form, refractivity N is used ($N=[n-1]*10^6$). In a wave front, the phase velocity is inversely proportional to n, so the speed of the signal components increase with height resulting in a downward bending of the beam path (anomalous propagation, or anaprop).

In the ideal case ($dN/dz=0$) the beam path is straight, whilst in a standard atmosphere where $dN/dz<0$ (yet the value is small) the path is a little curved. With higher values of dN/dz, the curvature of the radar wave increases to the extent that it may become comparable with earth curvature (temperature gradient of 13k/100m or a water pressure gradient of -3mb/100m [CEC, 1985]). It is convenient at this stage to introduce a second differential dM/dz where M is modified refractivity ($M=N+157z$) to account for earth curvature such that the Earth now appears flat with respect to the propagation paths of the radar waves. In the case where $dM/dz<0$ the radar waves are bent towards the surface of the Earth forming a 'duct'. In the latter case abnormal amounts of ground clutter are observed, due both to an increase in clutter from prone areas, and also from areas that are usually clutter free (van Gorp calls this 'inversion ground clutter', thereby differentiating between instances when anaprop does and does not produce increased ground clutter). Large moisture gradients (hydrolapses) are the dominating factor, marked temperature inversions making a less important contribution, and pressure gradient being the least important.

The classes of beam propagation are illustrated in figure 3.5.

When inversion clutter is observed it may be limited to certain regions and even to narrow sectors of the radar (areas most prone to inversion clutter are regions of rising ground facing the radar, whilst those completely free are often in the lee). In addition, the intensity of ground echoes due to anaprop usually varies in both space and time. Over land inversion clutter results in a speckled display of mosaic structure with apparent large intensity gradients across adjacent grid squares: van Gorp (1989) reports on a peculiar circular pattern. Onset and cessation of anaprop echoes is often rapid, for example, the appearance of possible intense echoes during the formation of a night-time inversion may take place with 30 minutes or so of inversion formation.

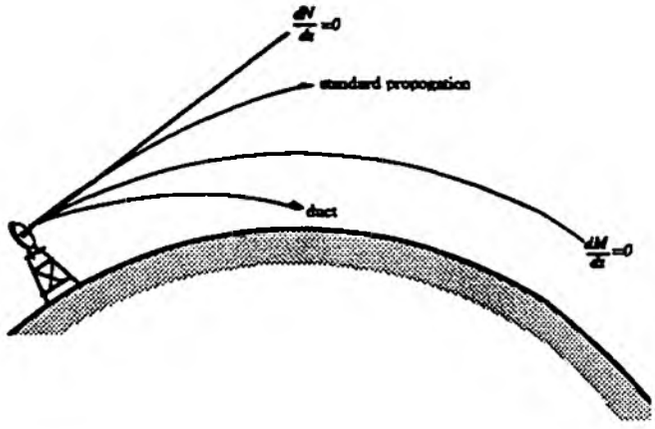

Figure 3.5: Refractive atmospheric propagation classification categories (after van Gorp, 1989)

Anaprop is most common in anticyclonic or warm sector conditions, beneath marked temperature inversions, and is often enhanced overnight during the development or intensification of the inversion. Generally little precipitation occurs during anticyclonic situations making the two echo types easier to distinguish (Smith, 1984a), although the two may exist together, for example, (Massambani, 1989) at the end of an anticyclonic spell (or possibly warm sector conditions), when a subsidence inversion persists until the arrival of a cold front. Anaprop may also be observed (though less frequently) in cyclonic conditions (usually in spring or summer) when very dry air is present above moist air at low levels (these atmospheric conditions are conducive to widespread rain making reflections due to rainfall and those due to anaprop difficult to differentiate). The height of the hydrolapse / inversion is important, anaprop being most likely when it is about 100 m above the radar. Anaprop becomes more unlikely with higher inversions, and rarely occurs when the inversion is more than about 1200 m above the radar. Anaprop will not occur when the radar beam is above the hydrolapse/inversion.

Although considerable progress has been made in the development of algorithms to detect and correct for inversion clutter, significant research effort is still being expended in this domain. As yet no procedure is perfect. In the U.K. a procedure developed by Smith (1981, 1984a, 1984b), (itself based on a procedure developed by Nicholas *et al* [1981]) has been operationally applied. The technique utilised attempts to map inversion clutter susceptibility for each cell within the radar coverage cartesian grid, as determined from an analysis of archived historical data. Each cell in the map has an integer value from 0 (never affected), through 1 (only affected by severe anaprop conditions), and 2 (affected by moderate anaprop conditions, to 3 (affected by slight anaprop conditions). According to anaprop severity, the likelihood of inversion clutter at any given location can be determined and an appropriate correction applied. The disadvantage is the technique is that skilled user intervention is required to specify the anaprop severity.

3.4. Factors due to Uncertainty in Physical Aspects

3.4.1. Z-R Relationship

The *Z-R* relationship (section 2.1) depends upon the particle size distribution of the raindrops, snowflakes and hailstones within the radar beam volume (because the reflectivity, *Z* is proportional to the sum of the sixth power of the particles diameters). Because the size and distribution of these within a given volume varies considerably, both within storms and from one precipitation type to another, the *a*, and *b* parameters can vary considerably (both temporally and spatially). A number of microphysical and kinematic processes affect the drop-size distribution and the speed at which the precipited drops fall including collision and coalescence, evaporation, downdraft and updraft. Battan (1973) lists over 60 different relationship between *Z* and *R*, though those given by Joss et al. (1970) cover the range of most of those published. These are:

$Z = 140 R^{1.5}$ for orographic rain and drizzle
$Z = 250 R^{1.5}$ for stratiform rain
$Z = 500 R^{1.5}$ for thunderstorm rain

The importance of the *a* and *b* parameters in the *Z-R* relationship is best illustrated by considering that for the parameter ranges listed by Battan, rainfall could be incorrectly assessed by a factor of 10 or more. The selection of the appropriate constants therefore constitutes the major problem in the estimation of precipitation by radar, and though various workers have reported indication of systematic variation in the *Z-R* relationship under some circumstances (for example Wilson and Brandes [1979] observed that generally *a* increases and *b* decreases with increasing convective intensity), this does not provide a realistic route for improved precipitation estimation. One solution, commonly used is to apply fixed values of *a* and *b*. Such a relation is likely to perform satisfactorily on average, but to be less representative in extreme types of rainfall. The most universally adopted relationship is the Marshall-Palmer relationship for homogeneous rainfall and stratified events which is of the form:

$Z = 200 R^{1.6}$

This Z-R relationship has been widely adopted throughout the world and is used by the U.K Meteorological Office in stratiform rainfalls. In the U.K. the relationship is updated in real-time (i.e. the *a* value is adjusted) with reference to a small number (typically 4-6) of ground-based telemetering raingauges.

3.4.2. Bright-Band

In conditions of little vertical mixing e.g. in frontal precipitation and away from the cores of convective cells in shower situations, hydrometeors present in the atmosphere become vertically

stratified according to the temperature structure of the atmosphere. At cloud top level where the temperature is well below freezing there are small ice particles which produce low radar reflectivities. As these particles fall through the cloud, the temperature increases, the particles aggregate and begin to melt, first becoming an ice core covered in a film of water before collapsing into raindrops. As water is much more reflective than ice (about five times), there is a large increase in the radar return as the particles begin to melt followed by a decline as their size decreases and fall speed increases. The bright-band layer usually lies about 300 m below the 0°C isotherm (various workers), the whole melting process generally taking place over a layer only a few hundred metres thick (Battan, 1973).

Bright-band is observed when the radar beam intersects the melting layer. Enhancement caused by the melting has a very marked effect on the radar return. Typically the enhancement in radar reflectivity signal in the bright-band over that in the rain below is a factor of 2 to 5 but it can be as large as 10. The extent to which precipitation estimation is affected depends on the proportion of the beam filled by the melting layer: for this reason bright-band is more of a problem at near range than at longer ranges where the beam volume is notably larger and the proportion filled smaller.

In an idealised form, a bright-band will be observed on a PPI display as a ring of enhanced radar returns centred on the radar at a range depending on the height of the melting layer and the elevation of the radar beam. In practice however, a well defined annulus is rarely observed and it is often broken or incomplete. Bright-band is most easily identified with high beam elevations where the radar beam 'cuts through' the melting layer at an acute angle; for longer ranges and lower beam elevations the effect is spread out radially and consequently more difficult to discern.

The effect of bright-band is shown schematically in figure 3.6. The profile of radar reflectivity with height shows a pronounced peak in the region of the melting layer. The graph of apparent rainfall rate against range assuming the rain is horizontally homogeneous, shows the same peak as the two beams pass through the bright-band but with the effect spread out over a wide range (which is dependent on the beam elevation). The figure also demonstrates how for a radar operating in PPI mode, a uniform bright-band of constant altitude present throughout the radar coverage may only be observed at few distinct ranges (range repetition).

The effects of the processes described both individually and resultant was studied theoretically by Austin and Bemis (1950). The result of their study is summarised in figure 3.7: the figure shows that if a falling frozen precipitation had a reflectivity of unity at the 0° isotherm, its value would have increased to 20 at 300 m below the melting level and then decrease rapidly to 5 at about 360 m where the frozen particles would be melted completely.

Lhermitte and Atlas (1963) made a number of observations using a vertically pointing X-band radar. The relationship they observed between particle fall speed and reflectivity is shown in figure 3.8. The figure shows a number of distinct layers, typifying the vertical reflectivity profile when a bright-band is present:

- *level 1*: this region represents the increasing return due to aggregation of snowflakes. Reflectivity increases with decreasing height.
- *level 2*: this represents the gradual melting of the particles with reflectivity increasing to its maximum value with decreasing height.
- *level 3*: in this layer, the fall speed of the particles is increasing and their size diminishing.

This causes the reflectivity to decrease from its maximum value with decreasing height.

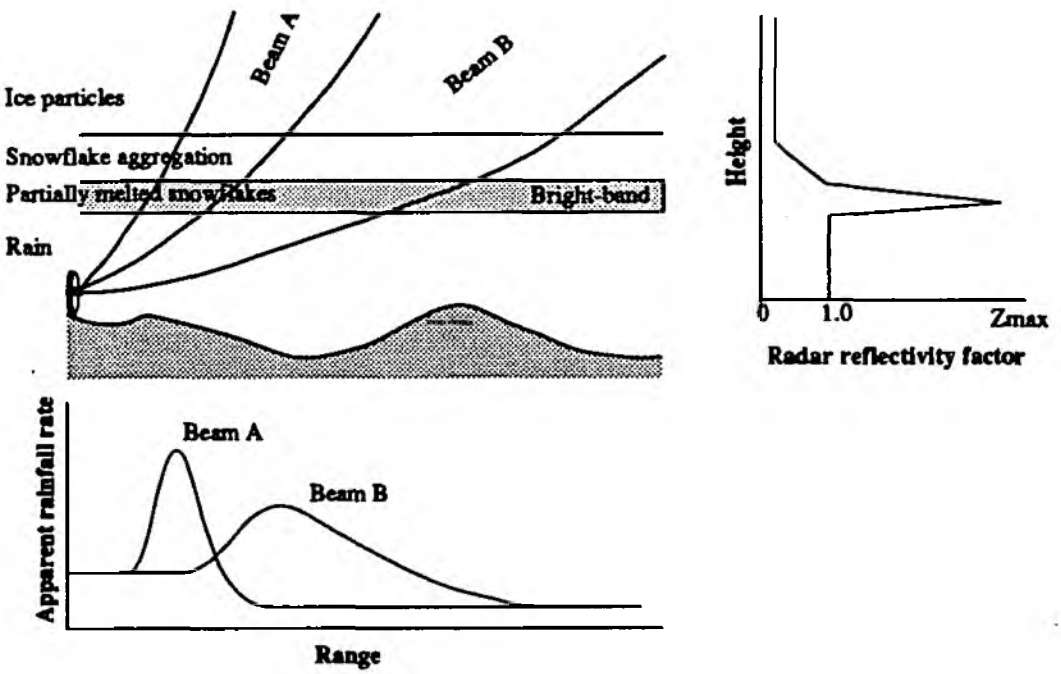

Figure 3.6: Schematic illustration of the effect of bright-band on the radar rainfall data (adapted from Smith, 1986)

Recent research conducted at the radar meteorology laboratory at McGill University, Montreal, (Canada) has provided new insights into bright-band phenomena. The occurrence distribution of bright-band layer thickness observed in the region is shown in figure 3.9. The figure shows that the layer rarely exceeds 800 m thickness, is usually at least 300 m thick, and is most commonly of the order 350 to 500 m deep. Pilot research with a vertically pointing radar system has enabled the relationship between bright-band layer thickness, and rainfall intensity below to be observed. The relationship is shown graphically for a combination of six storms in figure 3.10.

The major limitation of scanning radars as regards bright-band detection and correction is that the vertical resolution is usually inadequate, even quite close to the radar. For example a 1° beamwidth system at 50 km range will have a vertical resolution of 1000 m, clearly inadequate when the bright-band layer may be as little as 200 to 300 m thick. In addition, the bright-band may fall above

or below the radar beam at any particular location. The potential of high resolution vertical pointing (non scanning) radars for studying the vertical reflectivity profile and therefore bright-band dynamics is considerable.

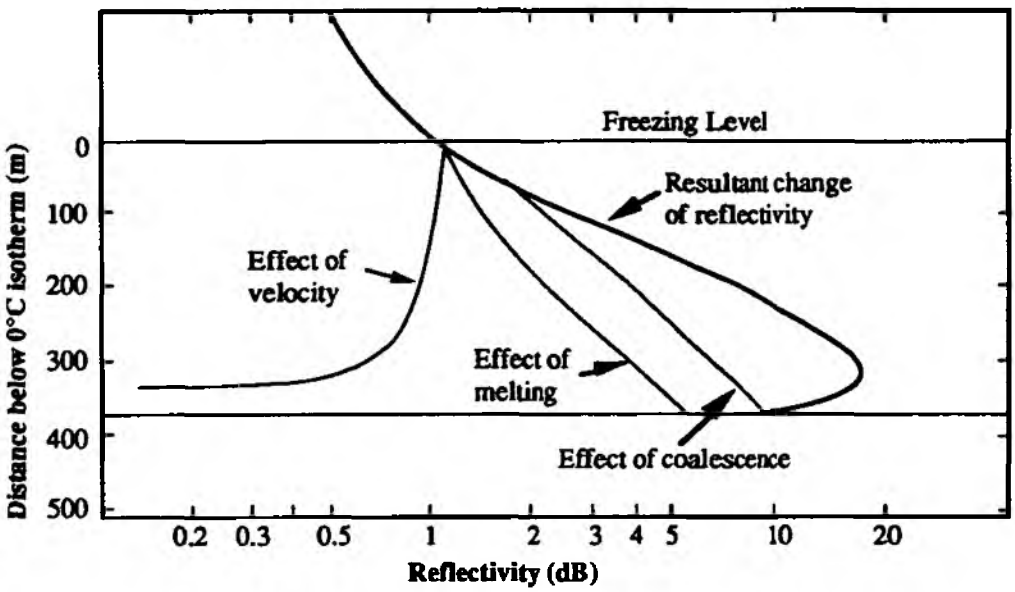

Figure 3.7: Effect of particle coalescence, melting and changes in the terminal velocity on radar reflectivity through the bright-band (adapted from Austin and Bemis, 1950)

The bright-band problem is most acute during frontal precipitation of moderate intensities, a condition which is commonly experienced in temperate latitudes during winter months. In these conditions in the U.K bright-band will occur close to the radar within the range where radar rainfall estimates are considered to be reliable for quantitative use (i.e. < 75 km). A number of different approaches have been tried in order to correct for bright-band errors. In the U.K the approach has centred on a software detection/correction algorithm developed by the Meteorological Office which aims to reduce the overall effect of the bright-band (rather than meticulously cancelling every minor error). The technique comprises of a detection component followed by correction. Detection utilises data from two elevated beams (often 1.5° and 2.5°, but dependent on radar), and is limited to heights from 350 m to 3000 m above the radar. A thorough review is provided by Smith (1986) and the reader is referred to this paper for further information. The detection component of the algorithm is operating routinely at most radar sites (including Chenies and Ingham) and appears reliable.

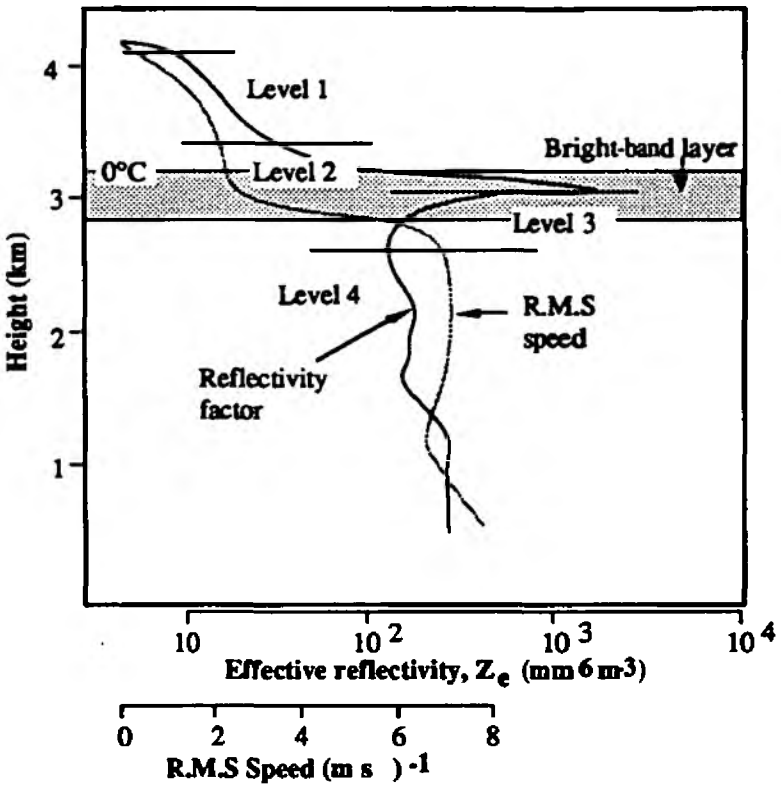

Figure 3.8: Profiles of reflectivity and root mean square particle fall speed in light (1 mm/hr) steady precipitation with a bright-band (Lhermitte and Austin, 1963)

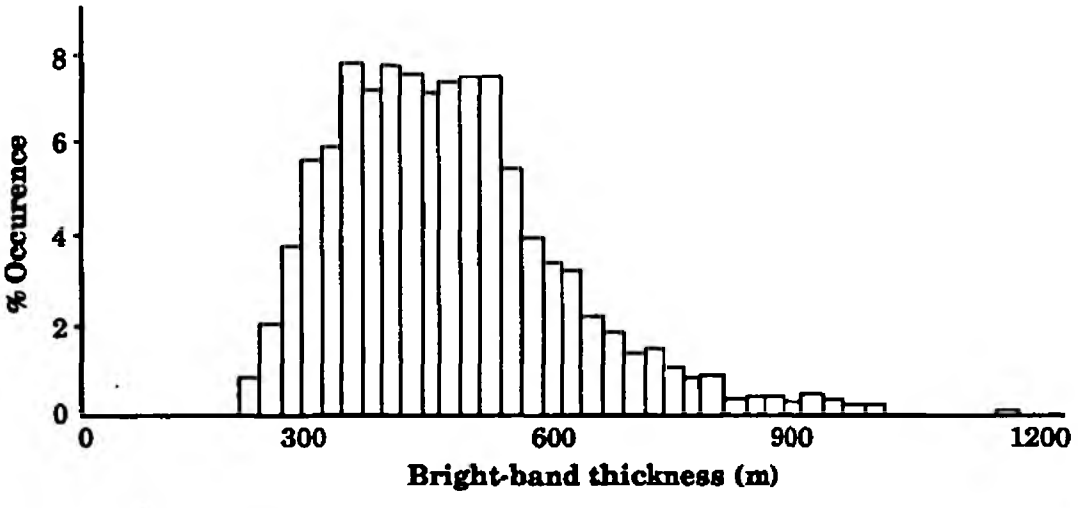

Figure 3.9: Distribution function of bright-band thickness for rainfalls with rainfall intensity exceeding 0.2 mm/hr for six storms during October and November 1989

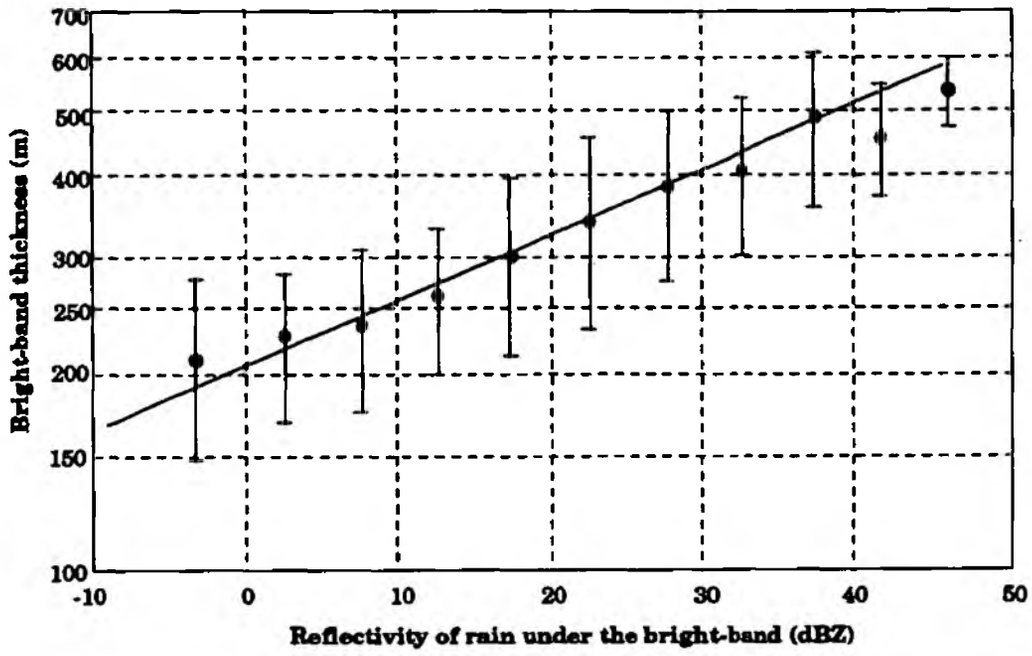

Figure 3.10: Bright-band layer thickness as a function of rainfall intensity below for six storms during October and November 1989

Chapter 4. Concluding Comments

This report has introduced some of the basic principles of weather radar observation of precipitation, and, in some detail, factors related to and affecting the accuracy with which precipitation can be quantitatively estimated using weather radar. An attempt has been made to classify the factors according to the manner in which they influence estimation. In practice it is often very difficult if not impossible to differentiate between the individual processes at work and the extent of their contribution: at best only to identify one or two of the dominant processes and quantify the extent to which these influence the final estimation.

It is important that users of radar data (particularly those responsible for quantitative application of radar data) have some knowledge of the underlying principles and the factors influencing quantitative data accuracy, so that the limititations (and strengths) of the data are known.

Some of the factors are more important for hydrological utilisation of the precipitation estimates than others. Often there is little or nothing that an end-point data user can do since the factors are beyond control. In the case of hardware related factors, the user must assume that the radar system is stable and has been designed in accordance with the physical conditions that prevail in the region. These assumption are usually fair and valid: a range of radar platforms are now manufactured designed solely for hydrometeorological applications in particular climatological regions (e.g. see ARIP Report 5 [Appendix 2], Collier, 1989, or Lawler, 1989). Radar hardware technology is now such that with careful hardware calibration, reflectivity is invariably measured with a high degree of precision and accuracy, the problem is in the conversion of the reflectivity values to rainfall intensities.

The material introduced should be regarded as complementary to that in ARIP Report 5, the report in which the results of an investigation into radar performance over the Anglian Region, and the development of a local adjustment procedure is described.

References

Andersson, T., (1989) 'Corrections for the partial blocking of the radar beam', *Proc, Int. Symp. on Hydrological Applications of Weather Radar*, Salford, U.K., August. (In Hydrological Applications of Weather Radar, Ed. Cluckie, I.D. and Collier, C.G., Ellis Horwood, U.K, 1990).

Austin, P.M., and Bemis, A.C. (1950) 'A quantitative study of the "bright-band" in radar precipitation echoes', *J. Meteorol.*, 7, 145-151.

Battan, L.J. (1973) *Radar Observation of the Atmosphere*, University of Chicago Press, Chicago, 324pp.

CEC (Commission of European Communities). (1985) 'Measurement of precipitation by radar', COST-72 Final Report, Report No. EUR 10171 EN, Luxembourg.

Collier, C.G. (1989) *Applications of Weather Radar Systems: A Guide to Uses of Radar Data in Meteorology and Hydrology*, Ellis Horwood Ltd., 294pp.

Collinge, V.K. (1989) 'Weather radar calibration in real time - prospects for improvement', *Proc, Int. Symp. on Hydrological Applications of Weather Radar*, Salford, U.K., August. (In Hydrological Applications of Weather Radar, Ed. Cluckie, I.D. and Collier, C.G., Ellis Horwood, U.K, 1990).

East, T.W.R., and Dore, B.V. (1957) 'An electric constant altitude display', *Proc. Sixth Weather Radar Conf.*, Amer. Met. Soc., 325-330.

Galli, G., and Joss, J. (1989) 'Using and adjusting conventional reflectivity data for estimation of precipitaion: past present and future studies in Switzerland', *Preprints, Int. Symp. on Hydrological Applications of Weather Radar*, Salford, U.K., August.

Giguere, A., and Austin, G.L. (1989) 'On the significance of radar wavelength in the estimation of snowfall', *Proc, Int. Symp. on Hydrological Applications of Weather Radar*, Salford, U.K., August. (In Hydrological Applications of Weather Radar, Ed. Cluckie, I.D. and Collier, C.G., Ellis Horwood, U.K, 1990).

Grayman, W.M., and Eagleson, P.S. (1970) 'A review of the accuracy of radar and raingauges for precipitation measurement', Hydrodynamics Laboratory Rep. No. 119, Massachusetts Institute of Technology.

Haggett, C. M. (1989) 'Weather radar for flood warning', Weather Radar and the Water Industry, British Hydrological Society, Occassional Paper No. 2.

Hamazu, K., and Wakabayashi, M. (1989) 'Ground clutter rejection for weather radar and weather doppler radar', *Proc, Int. Symp. on Hydrological Applications of Weather Radar*, Salford, U.K., August. (In Hydrological Applications of Weather Radar, Ed. Cluckie, I.D. and Collier, C.G., Ellis Horwood, U.K, 1990).

Harrold, T.W., English, E.J., and Nicholass, C.A. (1974) 'The accuracy of radar derived rainfall measurements in hilly terrain', *Q.J.R. Meteorol. Soc.*, **100**, 331-350.

Hudlow, M.D., Smith, J.A., Walton, M.L., and Shedd, R.C., (1989) 'NEXRAD-New era in hydrometeorology in the United States', *Proc, Int. Symp. on Hydrological Applications of Weather Radar*, Salford, U.K., August. (In Hydrological Applications of Weather Radar, Ed. Cluckie, I.D. and Collier, C.G., Ellis Horwood, U.K, 1990).

Joss, J., Schran, K., Thoms, J.C., and Waldvogel, A. (1970) *On the Quantitative Determination of Precipitation by Radar*, Wissenschaftclich Mitfeilung No. 63, Eidgenossischen Komnission Sum Studiumder Hagelgilbung und der Hergelsher, 38 pp.

Joss, J., and Waldvogel, A. (1989) 'Precipitation measurement and hydrology. A review', *Battan Memorial and Radar Conf.*, American Meteorological Society, Boston, Mass.

Lawler, K. P. (1989) 'Weather radar system design', *In Weather Radar and the Water Industry: Opportunities for the 1990's*. British Hydrological Society Occassional Paper No. 2, pp 14-23.

Lhermite, `R.M., and Atlas, D. (1961) 'Precipitation motion by pulse Doppler radar', *Proc. NinthWeather Radar Conf.*, Amer. Met. Soc., 218-223.

Marshall, J.S., and Palmer, W.M.K. (1948) 'The distribution of raindrops with size', *J. Meteorol.*, **5**, 165-166.

Marshall, J.S. (1957) 'The constant altitude presentation of radar weather patterns', *Proc. Sixth Weather Radar Conf.*, Amer. Met. Soc., 325-330.

Massambani, O., and Filho, A.J.P. (1989) 'The diurnal evolution of the ground return intensities and its use as a radar calibration procedure', *Proc, Int. Symp. on Hydrological Applications of Weather Radar*, Salford, U.K., August. (In Hydrological Applications of Weather Radar, Ed. Cluckie, I.D. and Collier, C.G., Ellis Horwood, U.K, 1990).

Nicholas, C.A., Palmer, S.G., and Haylock, S.A. (1981) 'A method for combining daily areal rainfall estimates and raingauges', Met O 8, Rainfall Memorandum No. 34, (unpublished), Bracknell.

Shedd, R.C., Smith, J.A., and Walton, M.L. (1989) 'Sectorised hybrid scan strategy of the NEXRAD precipitation processing system', *Proc, Int. Symp. on Hydrological Applications of Weather Radar*, Salford, U.K., August. (In Hydrological Applications of Weather Radar, Ed. Cluckie, I.D. and Collier, C.G., Ellis Horwood, U.K, 1990).

Smith, C.J. (1981) 'Spurious echoes observed by the Meteorological Office radar network and methods of reducing their intensity', Meteorological Office Radar Research Laboratory, Research Report No. 27, (unpublished).

Smith, C.J. (1984a) 'The removal of anaprop echoes from radar data', Met O 8, Rainfall Memorandum No. 61, (unpublished), Bracknell.

Smith, C.J. (1984b) 'The performance of the anaprop detection algorithm on Camborne, Clee and Upavon radar data', Met O 8, Rainfall Memorandum No. 65, (unpublished), Bracknell.

Smith, C.S. (1986) 'The reduction in errors caused by bright-bands in quantitative rainfall measurements made using radar', *J. Atmos. Ocean. Technol.*, **3**, 129-141.

Tateya, K., Nakatsugawa, M., and Yamada, T. (1989) 'Observation and simulation of rainfall in mountainous areas', *Proc, Int. Symp. on Hydrological Applications of Weather Radar*, Salford, U.K., August. (In Hydrological Applications of Weather Radar, Ed. Cluckie, I.D. and Collier, C.G., Ellis Horwood, U.K, 1990).

Treussart, H. (1968) *Le Radar Capteur Hydrologique*, La Meteorologie, 5th Series, No. 7, Societe Meteorologique de France, Paris (in French).

Van den Assem, S. (1989) 'Calibration of weather radar data in the Netherlands', *Proc, Int. Symp. on Hydrological Applications of Weather Radar*, Salford, U.K., August. (In Hydrological Applications of Weather Radar, Ed. Cluckie, I.D. and Collier, C.G., Ellis Horwood, U.K, 1990).

Van Gorp, J.J. (1989) 'Ground clutter reduction during rain measurement by a noncoherent radar system', COST

Wilson, J.W., and Brandes, E.A. (1979) 'Radar measurements of rainfall - a summary', *Bull. Am. Meteorol. Soc.*, **60**, 1048-1052.

Yuan, J. (1991) 'A comparison study of radar data resolutions and quantisation levels in the context of urban hydrology', North West Urban Radar Project Report No. 3, Water Resources Research Group, Department of Civil Engineering, University of Salford, 60pp (including appendices).